# Modeling of A Floating-Base Flexible Manipulator with Holonomic Constraints on The End-Effector

Tianming Wang, Wenjie Lu and Dikai Liu[1]

*Abstract*— **More and more applications of mobile robots demand intervention capabilities, compared to the widely used actively controlled rigid-link manipulators, passively controlled flexible-link manipulators have the advantages of lighter weight, higher operational speed, lower energy consumption and safer operation. However, the mobile robot with the flexible-link manipulator in contact situation has not gained much attention. In this paper, we derive a mathematical model of a floating-base flexible manipulator with the end-effector constrained at a fixed contact position using assumed mode method and quasi Lagrangian formulation. The proposed model is suitable for aerial or underwater intervention applications with the flexible link undergoing three-dimensional large bending deformation, and can be utilized to calculate contact force given external input force as well as pose and velocities of the robot. Comprehensive simulations and experiments were conducted for model validation, the test results provide material evidence to verify the model effectiveness.**

## I. INTRODUCTION

Mobile manipulators have gained extensive attention during the last decades due to their improved maneuverability and reduced power consumption over their rigid counterparts [1]. Interaction with environment is a main application for the mobile manipulators. Common interactive tasks, such as cable connecting, object catching, and parts replacing, only demand the rigid-link manipulator combined with the mobile platform. However, for some exploration tasks or scientific investigation work, there are usually a demand for the robot to control its end-effector to contact with the environment for sampling or detailed detection, but the mobile platform may have some movement during operation due to some external disturbances (wind or current). In this situation, the flexible-link manipulators can be a better choice as they can provide passive reaction, which is normally faster than the active reaction of the rigid-link manipulators. Thus, our research mainly focused on the floating-base flexible manipulator in constrained circumstance.

Flexible link manipulators have gained extensive attention during the last years due to their lightweight, higher operational speed, lower energy consumption and safer operation compared with the rigid-link manipulators [2], [3]. These advantages enable the flexible manipulators to be developed in variant fields, such as manufacturing industries [4] and aerospace industries [5], [6]. Accordingly, the necessity of analyzing the dynamic behavior of flexible link manipulators has been arisen, which attracted many researchers to explore. The most common dynamic modeling method is the Lagrangian formulation [7]–[11]. Chen [8] used the Lagrangian approach for dynamic modeling of multi-link flexible arms, the motion of each link is decomposed into a nominal rigid body motion and a deviation due to elastic deformations, while this is applicable only assuming small deformation. Abe [10] provided a model of a two-link rigid-flexible manipulator for large bending deformation, the method assumed the dynamic behavior is dominated by the first vibration mode. However, the high modes might also have some impacts on the overall system dynamics under some specific conditions. Chen and Huang [11] came up with a model of single-link flexible manipulators with an infinite number of vibration modes. Their modeling method benefits the precision motion control of the flexible manipulators.

Some complex tasks may need the flexible manipulators to interact with the environment. For example, thin and lightweight flexible arms have been used in minimally invasive surgery that make contact inside the patient's body [12], [13]. In atomic force microscopy, there would be interaction between a flexible microcantilever and the sample [14]. Thus, it is necessary to take the contact constraints into consideration when modeling. Plenty of work [15]–[18] still focused on the Lagrangian formulation, but the Lagrange multipliers was used to represent the contact forces and torques. Some researchers [19]–[24] derived the constrained equation of motion by applying Hamilton's principle and the Lagrange multiplier method. In these methods, the elastic deflections were normally assumed to be small. Smoljkic et al. [25] considered large deformations in flexible link, he provided a quasi-static model instead of a dynamic model for surgical cases where prudent operation is needed.

Existing work only considers fixed-base cases, while floating-base flexible manipulators seems more and more popular due to their improved manoeuvrability. However, modeling of these robots becomes more difficult, as the floating-base, like aerial robots or underwater robots, adds six degrees of freedom, making the traditional Lagrangian approach not effective any more. Thus, Meirovitch and Kwak [26] have proposed a quasi-Lagrangian formulation instead of standard Lagrangian formulation for modeling of a spacecraft with flexible appendages, this new method writes up the dynamics using body-fixed velocities, as the sensor information and actuator forces are exerted on body-fixed frame [20].

The mentioned research on the floating-base flexible manipulators only paid attention to unconstrained case, where the manipulator has a free-moving end-effector, very few work has been done on constrained case. Besides, most of the

[1]Authors are with Centre for Autonomous Systems, Faculty of Engineering and Information Technology, University of Technology Sydney, Ultimo, NSW 2007, Australia tianming.wang@student.uts.edu.au

above methods only considered small and planar deformation of flexible link, as motion and deformation of each link only occurs in the same direction of joint rotation. While the floating base has 6 DOF, the link deformation may occur in all directions, thus three-dimensional bending deformation occurs. And the existence of constrained surface will give rise to large bending deformation. However, there are also limited work that has been done in modeling under these situations.

This paper seeks a dynamic model of a floating-base flexible manipulator with the end-effector having contact with a point on the surface, thus holonomic constraints are considered. Assumed mode method and modified quasi Lagrangian formulation are used for model derivation, under the occurrence of three-dimensional large bending deformation of the flexible link. The developed model can be utilized to calculate contact force based on known external force and torque acting on the robot as well as pose and velocities of the robot. Also, using the model in controller design, the response could be faster than reading data from the force/torque sensor. Furthermore, comprehensive experiments have been designed for model validation.

In the following parts, Section 2 introduces problem formulation and several modeling assumptions. Section 3 provides detailed mathematical derivation of dynamic equations of motion. Then Section 4 presents experimental validation procedures and result analysis.

## II. PROBLEM FORMULATION

The robot introduced in this paper consists of a rigid body of size $L_x \times L_y \times L_z$ and a flexible link of length $L_a$, with the end-effector connected to the end of the link through an universal joint, as shown in Figure 1. The actuators mounted on the robot body (propellers or thrusters) are not shown here for simplification, but we consider the generalized force input to the system is generated by the thrusters or propellers. The flexible link is passive, and actuation comes from the rigid body. To describe the motion of the robot, we introduce a inertial frame $O-XYZ$ and a body-fixed frame $o-xyz$ centered at the robot body origin.

The contact can be well described by a stick and slip friction model [27]. However, the applications require the end-effector stays at a contact position for several seconds [28], therefore in this paper it is assumed that the end-effector is attached to the contact point. The resultant robot dynamic model and contact force calculated from it are effective in determining the contact condition (stick or slip).

The following assumptions are made for development of a dynamic model of the system.

- The flexible link can be considered as an Euler-Bernoulli beam, as the universal joint allows the link to rotate around the its neutral axis without twisting, thus the effects of shear deformation and rotary inertia can be neglected.
- The flexible link is of the first vibration mode.
- The universal joint is free from friction.

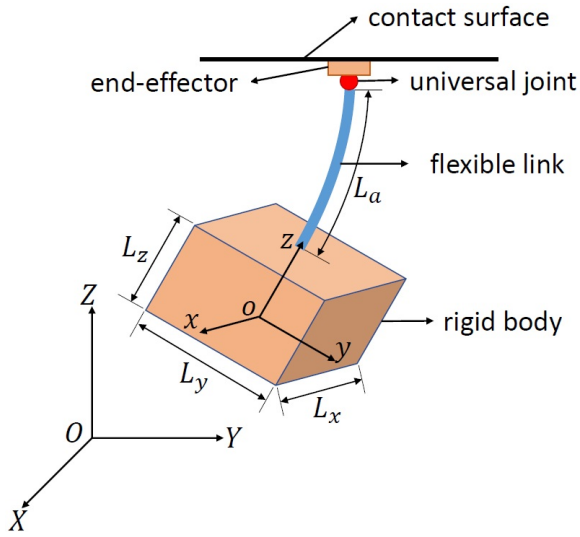


Fig. 1. Floating-Base Flexible Manipulator

## III. MATHEMATICAL MODELING

Quasi-Lagrangian formulation has been used for mathematical modeling. It should be noticed that the body-fixed velocity cannot be integrated to yield a set of generalized coordinates in terms of position and orientation, in fact, the integration has no immediate physical interpretation, thus the associated variables are referred to as quasi-coordinates, and the velocity components about the body axes can be regarded as quasi-velocities [29].

To define the generalized and quasi coordinates, we first need to define the rigid body pose vector in the inertial frame and the rigid body velocity vector in the body-fixed frame as

$$\boldsymbol{\eta} = \begin{bmatrix} \boldsymbol{R}_o & \boldsymbol{\theta} \end{bmatrix}^T, \quad \boldsymbol{\nu} = \begin{bmatrix} \boldsymbol{V}_o & \boldsymbol{\omega} \end{bmatrix}^T, \tag{1}$$

where $\boldsymbol{R}_o$ is the position of the origin of the body-fixed frame $o$ relative to the inertial frame $O-XYZ$ expressed in the inertial frame, and $\boldsymbol{\theta}$ is the angular displacements of $o-xyz$ relative to $O-XYZ$ expressed in the inertial frame. $\boldsymbol{V}_o$ is the velocity vector of $o$ and $\boldsymbol{\omega}$ is the angular velocity vector of axes $o-xyz$, both in terms of the body-fixed frame, they have the relationship

$$\boldsymbol{V}_o = \boldsymbol{J}_c \dot{\boldsymbol{R}}_o, \quad \boldsymbol{\omega} = \boldsymbol{J}_d \dot{\boldsymbol{\theta}}, \tag{2}$$

in which $\dot{\boldsymbol{R}}_o$ and $\dot{\boldsymbol{\theta}}$ are the velocity vector of $o$ and angular velocities in terms of the inertial frame. $\boldsymbol{J}_c$ is the rotation matrix expressing the transformation from the inertial frame to the body-fixed frame. $\boldsymbol{J}_d$ is the Jacobian to transform derivative of the Euler angles to body-fixed angular velocity. Both $\boldsymbol{J}_c$ and $\boldsymbol{J}_d$ depend on the angular displacements $\boldsymbol{\theta}$, the detailed expressions are given in Appendix A.

### A. Assumed Mode Method

Because of the difficulty to model such continuous dynamic systems with infinite number of degrees of freedom like the flexible link manipulators [30], some discretization methods have been utilized to represent the elastic deformation of the link. Three main methods exist in literature, which

are assumed mode method [31], finite element method [30], [32] and lumped parameter method [2], [33].

Our model used the assumed mode method, the dynamic behavior is expected to be dominated by the first vibration mode since the effect of the high-frequency modes is very small. With assumed mode characterization, the transverse elastic displacements $w$ can be expressed as the multiplication of space-dependent mode shape functions and time-dependent modal coordinates

$$w(s,t) = \phi(s)q(t), \tag{3}$$

where the variable $s$ is the coordinate along the deformed configuration of the flexible link, $\phi(s)$ and $q(t)$ represent mode shape functions and modal coordinates, respectively.

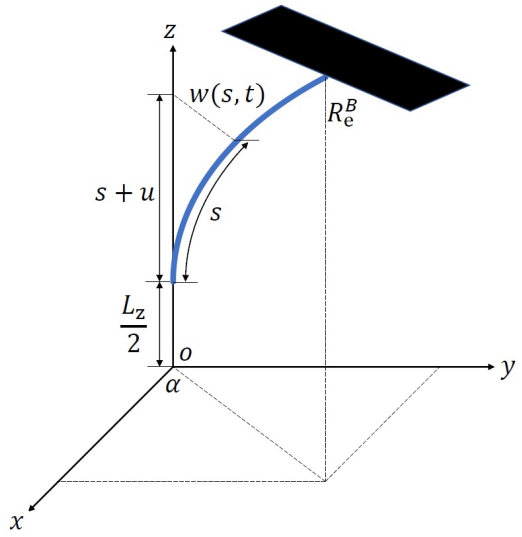


Fig. 2. Flexible Link in Body-Fixed Frame

As shown in Figure 2, the vector of the transverse elastic displacement in the body-fixed frame can be expressed as (the bold letters represent vectors in this paper)

$$\boldsymbol{w}^B = \begin{bmatrix} w\cos\alpha & w\sin\alpha & 0 \end{bmatrix}^T. \tag{4}$$

The bent flexible link is on a plane perpendicular to $x$-$y$ plane, the bending angle $\alpha$ is the angle between this plane and $x$-$z$ plane. And $u$ represents the axial shortening of the flexible link caused by large bending deformation. When elastic deformation occurs, it is assumed that the neutral axis of the flexible link is inextensional, hence $u$ can be derived based on the inextensibility condition [34] as

$$u(s) = -\frac{1}{2}q^2 \int_0^s \left(\frac{d\phi}{ds}\right)^2 ds. \tag{5}$$

In the maneuver, the degrees of freedom arise from the rigid-body translations and rotations of the platform and the elastic displacements of the flexible link. Thus, we can define the generalized coordinates and quasi velocities:

$$\boldsymbol{\delta} = \begin{bmatrix} \boldsymbol{R}_o & \boldsymbol{\theta} & q & \alpha \end{bmatrix}^T, \quad \boldsymbol{\mu} = \begin{bmatrix} \boldsymbol{V}_o & \boldsymbol{\omega} & \dot{q} & \dot{\alpha} \end{bmatrix}^T. \tag{6}$$

### B. Constraint Equations

The constraint condition is that the end-effector is attached to a fixed contact point, which can be described as

$$\boldsymbol{P}_C^I = \begin{bmatrix} X_C & Y_C & Z_C \end{bmatrix}^T. \tag{7}$$

As shown in Fig. 2, $\boldsymbol{R}_e^B$ represents the position of the flexible link's upper end point in body-fixed frame

$$\boldsymbol{R}_e^B = \boldsymbol{r}_e^B + \boldsymbol{w}_e^B = \begin{bmatrix} \phi(L_a)q\cos\alpha \\ \phi(L_a)q\sin\alpha \\ \frac{L_z}{2} + L_a + u(L_a) \end{bmatrix}, \tag{8}$$

where $\boldsymbol{r}_e^B$ is the nominal position of the end point in undeformed link relative to $o$, and $\boldsymbol{w}_e^B$ is the elastic displacement of the end point, both expressed in the body-fixed frame. The end point position in the inertial frame should be

$$\boldsymbol{R}_e^I = \boldsymbol{J}_c^T \boldsymbol{R}_e^B + \boldsymbol{R}_o. \tag{9}$$

When in contact, $\boldsymbol{R}_e^I$ and $\boldsymbol{P}_C^I$ should be equalized

$$\begin{aligned} \boldsymbol{R}_e^I &= \boldsymbol{P}_C^I \\ \boldsymbol{J}_c^T \boldsymbol{R}_e^B + \boldsymbol{R}_o - \boldsymbol{P}_C^I &= 0, \end{aligned} \tag{10}$$

this gives the constraint equations:

$$\boldsymbol{\Omega} = \boldsymbol{J}_c^T \boldsymbol{R}_e^B + \boldsymbol{R}_o - \boldsymbol{P}_C^I. \tag{11}$$

### C. Quasi Lagrangian Formulation

To derive quasi Lagrangian equations of motion, the Lagrange's equations in terms of generalized coordinates need to be given first

$$\frac{d}{dt}\left(\frac{\partial L}{\partial \dot{\boldsymbol{R}}_o}\right) - \frac{\partial L}{\partial \boldsymbol{R}_o} + \left(\frac{\partial \boldsymbol{\Omega}}{\partial \boldsymbol{R}_o}\right)^T \boldsymbol{\lambda} = \boldsymbol{f}_{v1}, \tag{12a}$$

$$\frac{d}{dt}\left(\frac{\partial L}{\partial \dot{\boldsymbol{\theta}}}\right) - \frac{\partial L}{\partial \boldsymbol{\theta}} + \left(\frac{\partial \boldsymbol{\Omega}}{\partial \boldsymbol{\theta}}\right)^T \boldsymbol{\lambda} = \boldsymbol{f}_{v2}, \tag{12b}$$

$$\frac{d}{dt}\left(\frac{\partial L}{\partial \dot{q}}\right) - \frac{\partial L}{\partial q} + \left(\frac{\partial \boldsymbol{\Omega}}{\partial q}\right)^T \boldsymbol{\lambda} = 0, \tag{12c}$$

$$\frac{d}{dt}\left(\frac{\partial L}{\partial \dot{\alpha}}\right) - \frac{\partial L}{\partial \alpha} + \left(\frac{\partial \boldsymbol{\Omega}}{\partial \alpha}\right)^T \boldsymbol{\lambda} = 0, \tag{12d}$$

where

$$L = T - U \tag{13}$$

is the Lagrangian in which $T$ is the kinetic energy and $U$ is the potential energy, $\boldsymbol{\Omega}$ and $\boldsymbol{\lambda}$ are the constraint equations and the Lagrange multipliers respectively, and the term $\boldsymbol{f}_{v1}$ and $\boldsymbol{f}_{v2}$ are the force and torque acting on the robot, in terms of the inertial frame.

According to the procedures described in Appendix B [35], the Lagrangian equations of motion in terms of quasi-

coordinates can be expressed as follows

$$\frac{d}{dt}\left(\frac{\partial T}{\partial \boldsymbol{V}_o}\right)+\tilde{\boldsymbol{\omega}}\frac{\partial T}{\partial \boldsymbol{V}_o}+\boldsymbol{J}_c\frac{\partial U}{\partial \boldsymbol{R}_o} +\boldsymbol{J}_c\left(\frac{\partial \boldsymbol{\Omega}}{\partial \boldsymbol{R}_o}\right)^T\boldsymbol{\lambda}=\boldsymbol{\tau}_{v1}, \tag{14a}$$

$$\frac{d}{dt}\left(\frac{\partial T}{\partial \boldsymbol{\omega}}\right)+\tilde{\boldsymbol{V}}_o\frac{\partial T}{\partial \boldsymbol{V}_o}+\tilde{\boldsymbol{\omega}}\frac{\partial T}{\partial \boldsymbol{\omega}}+(\boldsymbol{J}_d^T)^{-1}\frac{\partial U}{\partial \boldsymbol{\theta}} +(\boldsymbol{J}_d^T)^{-1}\left(\frac{\partial \boldsymbol{\Omega}}{\partial \boldsymbol{\theta}}\right)^T\boldsymbol{\lambda}=\boldsymbol{\tau}_{v2}, \tag{14b}$$

$$\frac{d}{dt}\left(\frac{\partial T}{\partial \dot{q}}\right)-\frac{\partial T}{\partial q}+\frac{\partial U}{\partial q}+\left(\frac{\partial \boldsymbol{\Omega}}{\partial q}\right)^T\boldsymbol{\lambda}=0, \tag{14c}$$

$$\frac{d}{dt}\left(\frac{\partial T}{\partial \dot{\alpha}}\right)-\frac{\partial T}{\partial \alpha}+\frac{\partial U}{\partial \alpha}+\left(\frac{\partial \boldsymbol{\Omega}}{\partial \alpha}\right)^T\boldsymbol{\lambda}=0, \tag{14d}$$

where the term $\boldsymbol{\tau}_{v1}$ and $\boldsymbol{\tau}_{v2}$ are the force and torque acting on the robot, in terms of the body-fixed frame. The relationship between generalized force in the body-fixed frame $\boldsymbol{\tau}_v$ and that in the inertial frame $\boldsymbol{f}_v$ is given in Appendix B.

Then we write the kinetic energy of the system

$$T=\frac{1}{2}m_r\boldsymbol{V}_o^T\boldsymbol{V}_o+\boldsymbol{V}_o^T\tilde{\boldsymbol{S}}_r^T\boldsymbol{\omega}+\frac{1}{2}\boldsymbol{\omega}^T\boldsymbol{I}_r\boldsymbol{\omega}, \tag{15}$$

where $m_r$ is the mass of the robot rigid body, $\tilde{\boldsymbol{S}}_r$ is a skew symmetric matrix of first moments of inertia and $\boldsymbol{I}_r$ is the inertia tensor. It should be noted that, in this paper, we assume the flexible link and end-effector are quite light compared to the rigid body, thus we neglect their mass in the calculation. The kinetic energy of the flexible link and end-effector can be considered as zero due to the ignorable mass.

The potential energy consists of two parts, elastic and gravitational. The elastic potential energy is expressed as [10]

$$U_E=\frac{EI}{2}q^2\int_0^{L_a}\left(\frac{d^2\phi}{ds^2}\right)^2ds+\frac{EI}{2}q^4\int_0^{L_a}\left(\frac{d^2\phi}{ds^2}\right)^2\left(\frac{d\phi}{ds}\right)^2ds. \tag{16}$$

By assuming the center of mass and the center of volume are the same for the robot rigid body, the gravitational potential energy can be written as

$$U_G=-m_r\boldsymbol{g}^T\boldsymbol{R}_o, \tag{17}$$

where $\boldsymbol{g}$ represents the acceleration of gravity.

Combining (16) and (17) together yields the total potential energy of the system

$$U=U_G+U_E. \tag{18}$$

Next, inserting (15), (18) and (11) into (14) and rearranging, we obtain the explicit Lagrange's equations in terms of quasi coordinates (matrix form is shown in Appendix C)

$$\begin{aligned}\boldsymbol{M}\dot{\boldsymbol{\mu}}+\boldsymbol{C}(\boldsymbol{\mu})\boldsymbol{\mu}+\boldsymbol{D}(\boldsymbol{\mu})\boldsymbol{\mu}+\boldsymbol{E}(\boldsymbol{\delta})+\boldsymbol{F}(\boldsymbol{\delta})\boldsymbol{\lambda}&=\boldsymbol{\tau}\\ \boldsymbol{M}\dot{\boldsymbol{\mu}}+\boldsymbol{N}(\boldsymbol{\mu},\boldsymbol{\delta})+\boldsymbol{F}(\boldsymbol{\delta})\boldsymbol{\lambda}&=\boldsymbol{\tau}.\end{aligned} \tag{19}$$

Then we calculate the second derivative of the constraint equations (11) (matrix form is shown in Appendix D)

$$\boldsymbol{A}(\boldsymbol{\delta})\dot{\boldsymbol{\mu}}+\boldsymbol{B}(\boldsymbol{\mu},\boldsymbol{\delta})=\boldsymbol{O}_{3\times1}. \tag{20}$$

Put (19) and (20) together, we can obtain the resultant Lagrange multipliers $\boldsymbol{\lambda}$, which is exactly the contact force that the end-effector applies to the constraint surface expressed in the inertial frame.

## IV. MODEL VALIDATION

### A. Experiment Platform

The following experiment platform is set in the Data Arena at UTS for validating the proposed robot dynamic model. As shown in Figure 3, the experiment platform consists of a robot body mock-up and a fixed aluminum stand. The mock-up consists of an aluminum cuboid body with a flexible link mounted on its top. The link is made of a polyurethane rod with length of 0.252 $m$. The upper end point of the link is connected to a universal joint, which is fixed on the aluminum stand through a force/torque sensor. This sensor is used for measuring the contact force.

On the bottom of the body, a handle connects to the body through another force/torque sensor, while the sensor readings are not exactly the external input force and torque, which are exerted on the rigid body's center of mass, thus there should be a mapping between the sensor readings and the external input force/torque. These force and torque are considered as the generalized force generated by the thrusters or propellers. Both sensors we use are Nano25 transducer from ATI Industrial Automation.

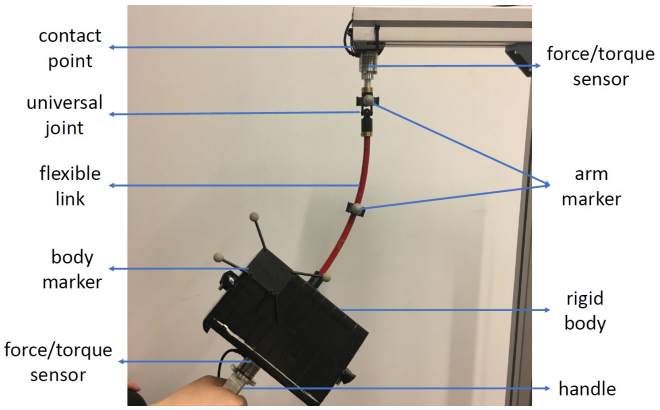


Fig. 3. Experiment Platform

Detailed parameters about the experiment setup are given as follows. The rigid body has a mass of 1.377 $kg$ and a cubic geometry of $0.171\times0.121\times0.110\ m^3$, its inertia moments with respect to the three coordinate axes of the body-fixed reference frame are 0.0041, 0.0061 and 0.0068 $kgm^2$, respectively. The flexible arm has the length of 0.252 $m$ and the diameter of 0.008 $m$, the flexural rigidity $EI$ is 6.8e-4 $Nm^2$.

As shown in Figure 3, IR reflective markers are fixed onto the mock-up. The markers and thus the rigid body and the flexible link are tracked by the OptiTrack motion capture system in the Data Arena. Figure 4 shows an image of the IR marker tracking during experiment, blue markers are attached to the metal stand which is always fixed on the ground,

yellow markers are attached to the cuboid body of the mock-up, and the orange markers are attached to upper end point and middle point of the flexible link.

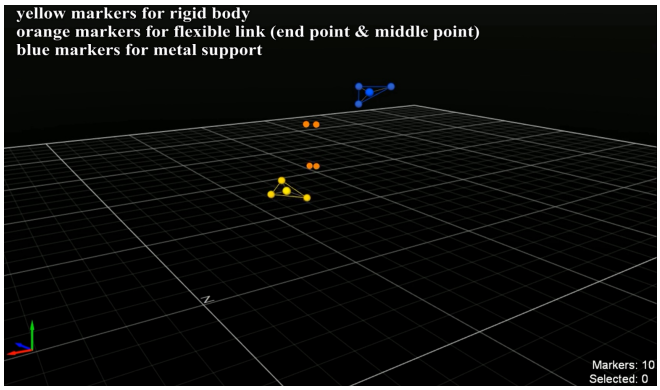


Fig. 4. An Image of OptiTrack Motion Capture System

### B. Experiment Results

During experiments, the handle is manually operated to introduce various motion of the rigid body and deformation of the flexible link, all of which are obtained through the OptiTrack motion capture system. At the meantime, the contact force (constrained force) and the input force and torque to the robot system are recorded. Then, given the acquired input force and torque, together with the body and arm pose and velocity, the contact force can be obtained from the developed model in Section 3.

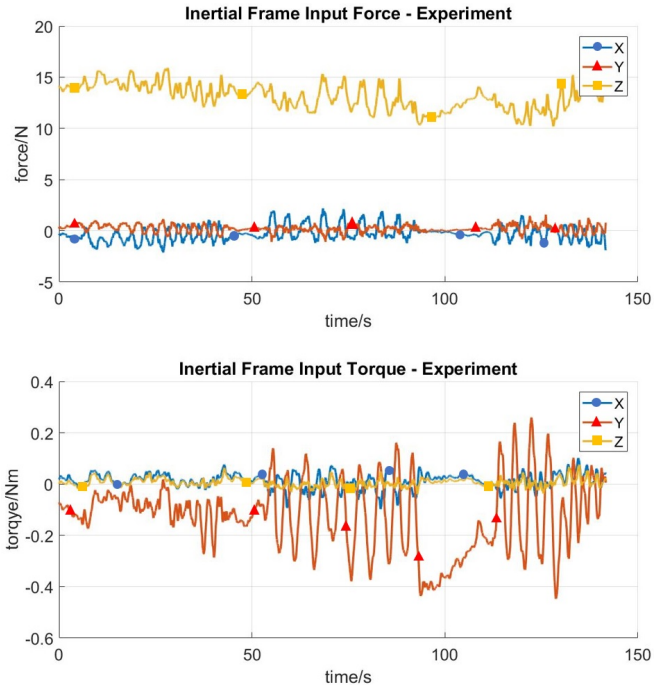


Fig. 5. External Input Force/Torque in Inertial Frame

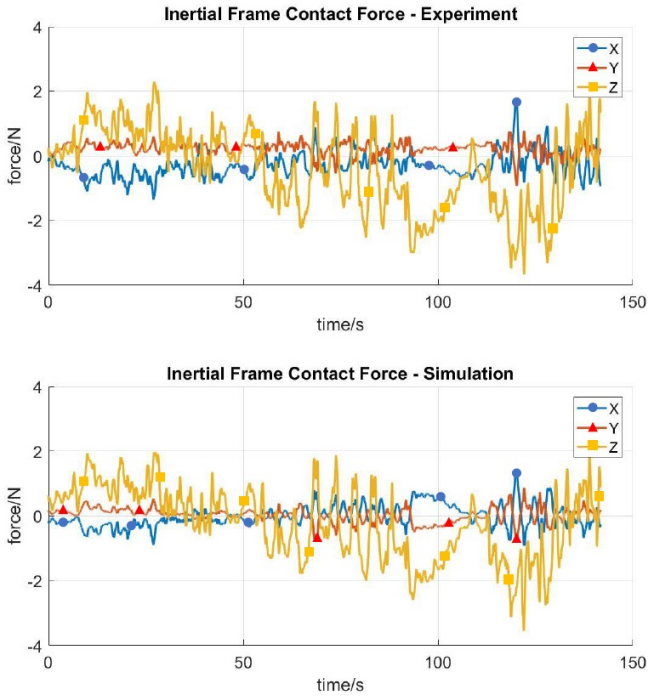


Fig. 6. Contact Force in Inertial Frame

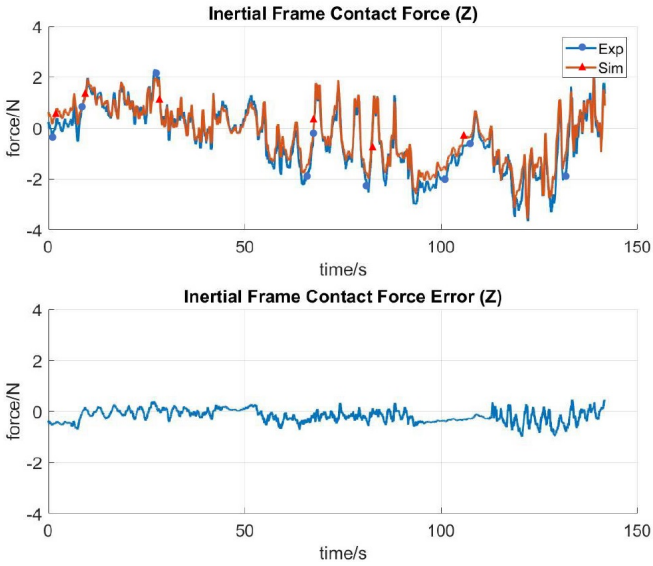


Fig. 7. Contact Force Error in Inertial Frame

Figure 5 shows the external input force and torque obtained from the force/torque sensor. And Figure 6 illustrates the contact forces measured by the force/torque sensor and calculated through the developed model, respectively. We mainly focus on the z-axis component of the contact force, the comparison results are shown in Figure 7. We can tell from this figure that, the contact forces of the experiment and simulation have nearly the same trend, and the error between them is sufficiently small (amplitude with in 0.8N). The results prove the effectiveness of the developed model.

## V. CONCLUSIONS

In this paper, we presented a mathematical modeling approach for the floating-base flexible manipulator with holonomic constraints on the end-effector. The assumed mode method and modified quasi Lagrangian formulation have been applied to derive the dynamic equations of motion, under the occurrence of three-dimensional large bending deformation of the flexible link. The contact force can be calculated using this model based on known external input force as well as pose and velocities of the robot. The simulation and experiment results have proven the effectiveness of the proposed model.

## APPENDIX

### A. Transformation Matrix

$\boldsymbol{J}_c$ is the rotation matrix between $o-xyz$ and $O-XYZ$, both $\boldsymbol{J}_c$ and $\boldsymbol{J}_d$ depend on the angular displacements $\boldsymbol{\theta}$, they are as follows:

$$\boldsymbol{J}_c = \begin{bmatrix} c\theta_2 c\theta_3 & c\theta_2 s\theta_3 & -s\theta_2 \\ s\theta_1 s\theta_2 c\theta_3 - c\theta_1 s\theta_3 & s\theta_1 s\theta_2 s\theta_3 + c\theta_1 c\psi & s\theta_1 c\theta_2 \\ c\theta_1 s\theta_2 c\theta_3 + s\theta_1 s\theta_3 & c\phi s\theta s\theta_3 - s\theta_1 c\psi & c\theta_1 c\theta_2 \end{bmatrix}, \tag{21a}$$

$$\boldsymbol{J}_d = \begin{bmatrix} 1 & 0 & -s\theta_2 \\ 0 & c\theta_1 & s\theta_1 c\theta_2 \\ 0 & -s\theta_1 & c\theta_1 c\theta_2 \end{bmatrix}, \tag{21b}$$

where $c\theta_i = \cos\theta_i$, $s\theta_i = \sin\theta_i$.

### B. Quasi Lagrangian Equations of Motion

The standard Lagrangian equations of motion in terms of generalized coordinates are

$$\frac{d}{dt}\left(\frac{\partial L}{\partial \dot{\boldsymbol{\eta}}}\right) - \frac{\partial L}{\partial \boldsymbol{\eta}} + \left(\frac{\partial \boldsymbol{\Omega}}{\partial \boldsymbol{\eta}}\right)^T \boldsymbol{\lambda} = \boldsymbol{f}_v, \tag{22a}$$

$$\frac{d}{dt}\left(\frac{\partial L}{\partial \dot{q}}\right) - \frac{\partial L}{\partial q} + \left(\frac{\partial \boldsymbol{\Omega}}{\partial q}\right)^T \boldsymbol{\lambda} = 0, \tag{22b}$$

$$\frac{d}{dt}\left(\frac{\partial L}{\partial \dot{\alpha}}\right) - \frac{\partial L}{\partial \alpha} + \left(\frac{\partial \boldsymbol{\Omega}}{\partial \alpha}\right)^T \boldsymbol{\lambda} = 0. \tag{22c}$$

According to the above, we have

$$\begin{bmatrix} \boldsymbol{V}_o \\ \boldsymbol{\omega} \end{bmatrix} = \begin{bmatrix} \boldsymbol{J}_c & \boldsymbol{O}_{3\times 3} \\ \boldsymbol{O}_{3\times 3} & \boldsymbol{J}_d \end{bmatrix} \begin{bmatrix} \dot{\boldsymbol{R}}_o \\ \dot{\boldsymbol{\theta}} \end{bmatrix} \tag{23}$$
$$\boldsymbol{\nu} = \boldsymbol{J}_a^T \dot{\boldsymbol{\eta}},$$

and, assuming that the matrix $\boldsymbol{J}_a$ is not singular, we can solve for the derivatives $\dot{\boldsymbol{\eta}}$ by writing

$$\dot{\boldsymbol{\eta}} = \boldsymbol{J}_b \boldsymbol{\nu}, \tag{24}$$

$$\boldsymbol{J}_a^T \boldsymbol{J}_b = \boldsymbol{J}_b^T \boldsymbol{J}_a = \boldsymbol{I}, \tag{25}$$

$$\boldsymbol{J}_b^T = \boldsymbol{J}_a^{-1} = \begin{bmatrix} \boldsymbol{J}_c & \boldsymbol{O}_{3\times 3} \\ \boldsymbol{O}_{3\times 3} & (\boldsymbol{J}_d^T)^{-1} \end{bmatrix}. \tag{26}$$

This enables us to express the kinetic energy as a function of the variables $\boldsymbol{\nu}$ instead of $\dot{\boldsymbol{\eta}}$. We denote this form of the kinetic energy by $\bar{T}(\boldsymbol{\nu}, q, \dot{q}, \alpha, \dot{\alpha})$, as opposed to the original form $T(\dot{\boldsymbol{\eta}}, q, \dot{q}, \alpha, \dot{\alpha})$. The potential energy $U$ will keep the original form as it does not include any items related to inertial frame velocities, so as $\boldsymbol{\Omega}$. Thus the new Lagrangian, which also include the variables $\dot{\boldsymbol{\nu}}$, will be in the form

$$\bar{L}(\boldsymbol{\eta}, \boldsymbol{\nu}, q, \dot{q}, \alpha, \dot{\alpha}) = \bar{T}(\boldsymbol{\nu}, q, \dot{q}, \alpha, \dot{\alpha}) - U(\boldsymbol{\eta}, q, \alpha). \tag{27}$$

Next we proceed to replace $\dot{\boldsymbol{\eta}}$ by $\boldsymbol{\nu}$ in the Lagrange's equations (22a)

$$\frac{\partial L}{\partial \dot{\eta}_k} = \sum_{i=1}^{n} \frac{\partial \bar{L}}{\partial \nu_i} \frac{\partial \nu_i}{\partial \dot{\eta}_k} = \sum_{i=1}^{n} a_{ki} \frac{\partial \bar{L}}{\partial \nu_i}, \quad k = 1, 2, ..., n, \tag{28}$$

where $a_{ij}$ is an element of matrix $\boldsymbol{J}_a$, it can clearly be written as the column matrix

$$\frac{\partial L}{\partial \dot{\boldsymbol{\eta}}} = \boldsymbol{J}_a \frac{\partial \bar{L}}{\partial \boldsymbol{\nu}}, \tag{29}$$

from which it follows that

$$\frac{d}{dt}\left(\frac{\partial L}{\partial \dot{\boldsymbol{\eta}}}\right) = \boldsymbol{J}_a \frac{d}{dt}\left(\frac{\partial \bar{L}}{\partial \boldsymbol{\nu}}\right) + \dot{\boldsymbol{J}}_a \frac{\partial \bar{L}}{\partial \boldsymbol{\nu}}. \tag{30}$$

Any element $a_{ij}$ of the square matrix $\dot{\boldsymbol{J}}_a$ has the form

$$\dot{a_{ij}} = \sum_{r=1}^{n} \frac{\partial a_{ij}}{\partial \eta_r} \dot{\eta}_r = \dot{\boldsymbol{\eta}}^T \frac{\partial a_{ij}}{\partial \boldsymbol{\eta}} = \boldsymbol{\nu}^T \boldsymbol{B}^T \frac{\partial a_{ij}}{\partial \boldsymbol{\eta}}, \tag{31}$$

which is a scalar. It must be noted here that the above triple matrix product $\boldsymbol{\nu}^T \boldsymbol{J}_b^T \frac{\partial a_{ij}}{\partial \boldsymbol{\eta}}$ does not involve summation over the indices of $a_{ij}$. Then we arrange the resulting scalars in the square matrix

$$\dot{\boldsymbol{J}}_a = \boldsymbol{\nu}^T \boldsymbol{J}_b^T \left[\frac{\partial \boldsymbol{J}_a}{\partial \boldsymbol{\eta}}\right]_1, \tag{32}$$

and we get

$$\frac{d}{dt}\left(\frac{\partial L}{\partial \dot{\boldsymbol{\eta}}}\right) = \boldsymbol{J}_a \frac{d}{dt}\left(\frac{\partial \bar{L}}{\partial \boldsymbol{\nu}}\right) + \boldsymbol{\nu}^T \boldsymbol{J}_b^T \left[\frac{\partial \boldsymbol{J}_a}{\partial \boldsymbol{\eta}}\right]_1 \frac{\partial \bar{L}}{\partial \boldsymbol{\nu}}. \tag{33}$$

Following the same pattern, we write

$$\begin{aligned} \frac{\partial L}{\partial \eta_k} &= \frac{\partial \bar{L}}{\partial \eta_k} + \sum_{i=1}^{n} \frac{\partial \bar{L}}{\partial \nu_i} \frac{\partial \nu_i}{\partial \eta_k} = \frac{\partial \bar{L}}{\partial \eta_k} + \sum_{i=1}^{n} \frac{\partial \bar{L}}{\partial \nu_i} \sum_{j=1}^{n} \frac{\partial a_{ij}}{\partial \eta_k} \dot{\eta}_j \\ &= \frac{\partial \bar{L}}{\partial \eta_k} + \dot{\boldsymbol{\eta}}^T \frac{\partial \boldsymbol{J}_a}{\partial \eta_k} \frac{\partial \bar{L}}{\partial \boldsymbol{\nu}} = \frac{\partial \bar{L}}{\partial \eta_k} + \boldsymbol{\nu}^T \boldsymbol{J}_b^T \frac{\partial \boldsymbol{J}_a}{\partial \eta_k} \frac{\partial \bar{L}}{\partial \boldsymbol{\nu}}, \end{aligned} \tag{34}$$

where this time summations over both indices of $a_{ij}$ are involved. However, there is no summation over the index in $\partial \eta_k$. This enables us to write the column matrix

$$\frac{\partial L}{\partial \boldsymbol{\eta}} = \frac{\partial \bar{L}}{\partial \boldsymbol{\eta}} + \boldsymbol{\nu}^T \boldsymbol{J}_b^T \left[\frac{\partial \boldsymbol{J}_a}{\partial \boldsymbol{\eta}}\right]_2 \frac{\partial \bar{L}}{\partial \boldsymbol{\nu}}, \tag{35}$$

where the triple matrix product $\boldsymbol{\nu}^T \boldsymbol{J}_b^T \left[\frac{\partial \boldsymbol{J}_a}{\partial \boldsymbol{\eta}}\right]_2$ produces $n$ row matrices, one for each $\partial \eta_k$. These $n$ row matrices are arranged in the square matrix premultiplying $\frac{\partial \bar{L}}{\partial \boldsymbol{\nu}}$.

Introduction of (33) and (35) into (22a) yields

$$\begin{aligned} &\left(\boldsymbol{J}_a \frac{d}{dt}\left(\frac{\partial \bar{L}}{\partial \boldsymbol{\nu}}\right) + \boldsymbol{\nu}^T \boldsymbol{J}_b^T \left[\frac{\partial \boldsymbol{J}_a}{\partial \boldsymbol{\eta}}\right]_1 \frac{\partial \bar{L}}{\partial \boldsymbol{\nu}}\right) - \\ &\left(\frac{\partial \bar{L}}{\partial \boldsymbol{\eta}} + \boldsymbol{\nu}^T \boldsymbol{J}_b^T \left[\frac{\partial \boldsymbol{J}_a}{\partial \boldsymbol{\eta}}\right]_2 \frac{\partial \bar{L}}{\partial \boldsymbol{\nu}}\right) + \left(\frac{\partial \boldsymbol{\Omega}}{\partial \boldsymbol{\eta}}\right)^T \boldsymbol{\lambda} = \boldsymbol{f}_v. \end{aligned} \tag{36}$$

Next premultiply through (36) by $\boldsymbol{J}_b^T$, we obtain

$$\frac{d}{dt}\left(\frac{\partial \bar{L}}{\partial \boldsymbol{\nu}}\right)+\boldsymbol{J}_b^T\boldsymbol{\Gamma}\frac{\partial \bar{L}}{\partial \boldsymbol{\nu}}-\boldsymbol{J}_b^T\frac{\partial \bar{L}}{\partial \boldsymbol{\eta}}+\boldsymbol{J}_b^T\left(\frac{\partial \boldsymbol{\Omega}}{\partial \boldsymbol{\eta}}\right)^T\boldsymbol{\lambda}=\boldsymbol{\tau}_v, \quad (37)$$

which are referred to as the Lagrangian equations of motion for quasi-coordinates, where

$$\boldsymbol{\Gamma}=\boldsymbol{\nu}^T\boldsymbol{J}_b^T\left[\frac{\partial \boldsymbol{J}_a}{\partial \boldsymbol{\eta}}\right]_1-\boldsymbol{\nu}^T\boldsymbol{J}_b^T\left[\frac{\partial \boldsymbol{J}_a}{\partial \boldsymbol{\eta}}\right]_2, \quad (38)$$

$$\boldsymbol{J}_b^T\boldsymbol{\Gamma}=\begin{bmatrix}\tilde{\boldsymbol{\omega}} & 0\\ \tilde{\boldsymbol{V}}_o & \tilde{\boldsymbol{\omega}}\end{bmatrix}, \quad (39)$$

in which $\tilde{\boldsymbol{\omega}}$ and $\tilde{\boldsymbol{V}}_o$ are skew-symmetric matrices corresponding to $\boldsymbol{\omega}$ and $\boldsymbol{V}_o$, respectively. And

$$\boldsymbol{\tau}_v=\boldsymbol{J}_b^T\boldsymbol{f}_v, \quad (40)$$

representing the generalized force in body-fixed frame.

The equation (36) can be further decomposed into two parts for $\boldsymbol{V}_o$ and $\boldsymbol{\omega}$ respectively, and (22b) and (22c) can be involved in the complete form of the quasi Lagrange's equations. Also, take (27) into consideration, the final equations will be

$$\begin{aligned}&\frac{d}{dt}\left(\frac{\partial \bar{T}}{\partial \boldsymbol{V}_o}\right)+\tilde{\boldsymbol{\omega}}\frac{\partial \bar{T}}{\partial \boldsymbol{V}_o}+\boldsymbol{J}_c\frac{\partial U}{\partial \boldsymbol{R}_o}\\ &\qquad+\boldsymbol{J}_c\left(\frac{\partial \boldsymbol{\Omega}}{\partial \boldsymbol{R}_o}\right)^T\boldsymbol{\lambda}=\boldsymbol{\tau}_{v1},\end{aligned} \quad (41a)$$

$$\begin{aligned}&\frac{d}{dt}\left(\frac{\partial \bar{T}}{\partial \boldsymbol{\omega}}\right)+\tilde{\boldsymbol{V}}_o\frac{\partial \bar{T}}{\partial \boldsymbol{V}_o}+\tilde{\boldsymbol{\omega}}\frac{\partial \bar{T}}{\partial \boldsymbol{\omega}}+(\boldsymbol{J}_d^T)^{-1}\frac{\partial U}{\partial \boldsymbol{\theta}}\\ &\qquad+(\boldsymbol{J}_d^T)^{-1}\left(\frac{\partial \boldsymbol{\Omega}}{\partial \boldsymbol{\theta}}\right)^T\boldsymbol{\lambda}=\boldsymbol{\tau}_{v2},\end{aligned} \quad (41b)$$

$$\frac{d}{dt}\left(\frac{\partial \bar{T}}{\partial \dot{q}}\right)-\frac{\partial \bar{T}}{\partial q}+\frac{\partial U}{\partial q}+\left(\frac{\partial \boldsymbol{\Omega}}{\partial q}\right)^T\boldsymbol{\lambda}=0, \quad (41c)$$

$$\frac{d}{dt}\left(\frac{\partial \bar{T}}{\partial \dot{\alpha}}\right)-\frac{\partial \bar{T}}{\partial \alpha}+\frac{\partial U}{\partial \alpha}+\left(\frac{\partial \boldsymbol{\Omega}}{\partial \alpha}\right)^T\boldsymbol{\lambda}=0. \quad (41d)$$

### C. Lagrangian Equations of Motion in Matrix Form

Lagrangian equations of motion in terms of quasi coordinates in matrix form:

$$\begin{aligned}&\begin{bmatrix} m_r\boldsymbol{I}_3+\boldsymbol{M}_{A1} & -\tilde{\boldsymbol{S}}_r & \boldsymbol{O}_{3\times1} & \boldsymbol{O}_{3\times1}\\ \tilde{\boldsymbol{S}}_r & \boldsymbol{I}_r+\boldsymbol{M}_{A2} & \boldsymbol{O}_{3\times1} & \boldsymbol{O}_{3\times1}\\ \boldsymbol{O}_{1\times3} & \boldsymbol{O}_{1\times3} & 0 & 0\\ \boldsymbol{O}_{1\times3} & \boldsymbol{O}_{1\times3} & 0 & 0\end{bmatrix}\begin{bmatrix}\dot{\boldsymbol{V}}_o\\ \dot{\boldsymbol{\omega}}\\ \ddot{q}\\ \ddot{\alpha}\end{bmatrix}\\ &+\begin{bmatrix} m_r\tilde{\boldsymbol{\omega}}+\tilde{\boldsymbol{\omega}}\boldsymbol{M}_{A1} & -\tilde{\boldsymbol{\omega}}\tilde{\boldsymbol{S}}_r & \boldsymbol{O}_{3\times1} & \boldsymbol{O}_{3\times1}\\ \tilde{\boldsymbol{S}}_r\tilde{\boldsymbol{\omega}}+\tilde{\boldsymbol{V}}_o\boldsymbol{M}_{A1} & \tilde{\boldsymbol{\omega}}\boldsymbol{I}_r+\tilde{\boldsymbol{\omega}}\boldsymbol{M}_{A2} & \boldsymbol{O}_{3\times1} & \boldsymbol{O}_{3\times1}\\ \boldsymbol{O}_{1\times3} & \boldsymbol{O}_{1\times3} & 0 & 0\\ \boldsymbol{O}_{1\times3} & \boldsymbol{O}_{1\times3} & 0 & 0\end{bmatrix}\begin{bmatrix}\boldsymbol{V}_o\\ \boldsymbol{\omega}\\ \dot{q}\\ \dot{\alpha}\end{bmatrix}\\ &+\begin{bmatrix}\boldsymbol{D}_{v1} & \boldsymbol{O}_{3\times3} & \boldsymbol{O}_{3\times1} & \boldsymbol{O}_{3\times1}\\ \boldsymbol{O}_{3\times3} & \boldsymbol{D}_{v2} & \boldsymbol{O}_{3\times1} & \boldsymbol{O}_{3\times1}\\ \boldsymbol{O}_{1\times3} & \boldsymbol{O}_{1\times3} & 0 & 0\\ \boldsymbol{O}_{1\times3} & \boldsymbol{O}_{1\times3} & 0 & 0\end{bmatrix}\begin{bmatrix}\boldsymbol{V}_o\\ \boldsymbol{\omega}\\ \dot{q}\\ \dot{\alpha}\end{bmatrix}\\ &+\begin{bmatrix}-m_t\boldsymbol{J}_c\boldsymbol{g}\\ \boldsymbol{O}_{3\times1}\\ EIqH_{\phi1}+2EIq^3H_{\phi2}\\ 0\end{bmatrix}\\ &+\begin{bmatrix}\boldsymbol{J}_c\\ (\boldsymbol{J}_d^T)^{-1}\boldsymbol{H}_{\theta2}\\ \boldsymbol{H}_{qe}^T\boldsymbol{J}_c\\ \boldsymbol{H}_{\alpha e}^T\boldsymbol{J}_c\end{bmatrix}\boldsymbol{\lambda}=\begin{bmatrix}\boldsymbol{\tau}_{v1}\\ \boldsymbol{\tau}_{v2}\\ 0\\ 0\end{bmatrix},\end{aligned} \quad (42)$$

where

$$\boldsymbol{H}_{qe}=\frac{\partial \boldsymbol{R}_e^B}{\partial q}=\begin{bmatrix}\phi_e\cos\alpha\\ \phi_e\sin\alpha\\ -q\int_0^{L_a}\left(\frac{d\phi}{ds}\right)^2ds\end{bmatrix}, \quad (43a)$$

$$\boldsymbol{H}_{\alpha e}=\frac{\partial \boldsymbol{R}_e^B}{\partial \alpha}=\begin{bmatrix}-\phi_e q\sin\alpha\\ \phi_e q\cos\alpha\\ 0\end{bmatrix}, \quad (43b)$$

$$\boldsymbol{H}_{\theta2}=\begin{bmatrix}\boldsymbol{R}_e^{BT}\left(\frac{\partial \boldsymbol{J}_c^T}{\partial \theta_1}\right)^T\\ \boldsymbol{R}_e^{BT}\left(\frac{\partial \boldsymbol{J}_c^T}{\partial \theta_2}\right)^T\\ \boldsymbol{R}_e^{BT}\left(\frac{\partial \boldsymbol{J}_c^T}{\partial \theta_3}\right)^T\end{bmatrix}, \quad (43c)$$

$$H_{\phi1}=\int_0^{L_a}\left(\frac{d^2\phi}{ds^2}\right)^2ds, \quad (43d)$$

$$H_{\phi2}=\int_0^{L_a}\left(\frac{d^2\phi}{ds^2}\right)^2\left(\frac{d\phi}{ds}\right)^2ds. \quad (43e)$$

### D. Second Derivative of Constraint Equations in Matrix Form

The second derivative of the constraint equations in matrix form:

$$\begin{aligned}&\begin{bmatrix}\boldsymbol{J}_c^T & -\boldsymbol{J}_cS(\boldsymbol{R}_e^B) & \boldsymbol{J}_c^T\boldsymbol{K}_1 & \boldsymbol{J}_c^T\boldsymbol{K}_2\end{bmatrix}\begin{bmatrix}\dot{\boldsymbol{V}}_o\\ \dot{\boldsymbol{\omega}}\\ \ddot{q}\\ \ddot{\alpha}\end{bmatrix}\\ &+\begin{bmatrix}\boldsymbol{J}_c^T\tilde{\boldsymbol{\omega}}\boldsymbol{V}_o+\boldsymbol{J}_c^T\tilde{\boldsymbol{\omega}}^2\boldsymbol{R}_e^B+2\boldsymbol{J}_c^T\tilde{\boldsymbol{\omega}}\dot{\boldsymbol{R}}_e^B+\boldsymbol{J}_c^T\boldsymbol{K}_3\end{bmatrix}=\boldsymbol{O}_{3\times1},\end{aligned} \quad (44)$$

where

$$\boldsymbol{K}_1 = \begin{bmatrix} \phi_e \cos\alpha \\ \phi_e \sin\alpha \\ -q\int_0^{L_a}\left(\frac{d\phi}{ds}\right)^2 ds \end{bmatrix}, \tag{45a}$$

$$\boldsymbol{K}_2 = \begin{bmatrix} -\phi_e q \sin\alpha \\ \phi_e q \cos\alpha \\ 0 \end{bmatrix}, \tag{45b}$$

$$\boldsymbol{K}_3 = \begin{bmatrix} -\phi_e(2\dot{q}\dot{\alpha}\sin\alpha + q\dot{\alpha}^2\cos\alpha) \\ \phi_e(2\dot{q}\dot{\alpha}\cos\alpha - q\dot{\alpha}^2\sin\alpha) \\ -\dot{q}^2\int_0^{L_a}\left(\frac{d\phi}{ds}\right)^2 ds \end{bmatrix}. \tag{45c}$$

## REFERENCES


[1] M. H. Korayem, S. Firouzy, and A. Heidari, "Dynamic load carrying capacity of mobile-base flexible-link manipulators: feedback linearization control approach," in *Robotics and Biomimetics, 2007. ROBIO 2007. IEEE International Conference on*. IEEE, 2007, pp. 2172–2177.

[2] S. K. Dwivedy and P. Eberhard, "Dynamic analysis of flexible manipulators, a literature review," *Mechanism and machine theory*, vol. 41, no. 7, pp. 749–777, 2006.

[3] C. T. Kiang, A. Spowage, and C. K. Yoong, "Review of control and sensor system of flexible manipulator," *Journal of Intelligent & Robotic Systems*, vol. 77, no. 1, pp. 187–213, 2015.

[4] W. Tao, M. Zhang, M. Liu, and X. Yun, "Residual vibration analysis and suppression for scara robot arm in semiconductor manufacturing," in *Intelligent Robots and Systems, 2006 IEEE/RSJ International Conference on*. IEEE, 2006, pp. 5153–5158.

[5] M. Gu and J.-C. Piedbœuf, "A flexible-arm as manipulator position and force detection unit," *Control engineering practice*, vol. 11, no. 12, pp. 1433–1448, 2003.

[6] J. De Carufel, E. Martin, and J.-C. Piedbœuf, "Control strategies for hardware-in-the-loop simulation of flexible space robots," *IEE Proceedings-Control Theory and Applications*, vol. 147, no. 6, pp. 569–579, 2000.

[7] M. A. Arteaga, "On the properties of a dynamic model of flexible robot manipulators," *Journal of dynamic systems, measurement, and control*, vol. 120, no. 1, pp. 8–14, 1998.

[8] W. Chen, "Dynamic modeling of multi-link flexible robotic manipulators," *Computers & Structures*, vol. 79, no. 2, pp. 183–195, 2001.

[9] B. Subudhi and A. S. Morris, "Dynamic modelling, simulation and control of a manipulator with flexible links and joints," *Robotics and Autonomous Systems*, vol. 41, no. 4, pp. 257–270, 2002.

[10] A. Abe, "Trajectory planning for residual vibration suppression of a two-link rigid-flexible manipulator considering large deformation," *Mechanism and Machine Theory*, vol. 44, no. 9, pp. 1627–1639, 2009.

[11] B. Chen and J. Huang, "Decreasing infinite-mode vibrations in single-link flexible manipulators by a continuous function," *Proceedings of the Institution of Mechanical Engineers, Part I: Journal of Systems and Control Engineering*, p. 0959651817708489, 2017.

[12] G. Dogangil, B. Davies, and F. Rodriguez y Baena, "A review of medical robotics for minimally invasive soft tissue surgery," *Proceedings of the Institution of Mechanical Engineers, Part H: Journal of Engineering in Medicine*, vol. 224, no. 5, pp. 653–679, 2010.

[13] M. Tavakoli and R. D. Howe, "Haptic effects of surgical teleoperator flexibility," *The International Journal of Robotics Research*, vol. 28, no. 10, pp. 1289–1302, 2009.

[14] A. Bazaei and M. Moallem, "Improving force control bandwidth of flexible-link arms through output redefinition," *IEEE/ASME Transactions On Mechatronics*, vol. 16, no. 2, pp. 380–386, 2011.

[15] L. Tian, J. Wang, and Z. Mao, "Constrained motion control of flexible robot manipulators based on recurrent neural networks," *IEEE Transactions on Systems, Man, and Cybernetics, Part B (Cybernetics)*, vol. 34, no. 3, pp. 1541–1552, 2004.

[16] S. Kilicaslan, M. K. Ozgoren, and S. K. Ider, "Control of constrained spatial three-link flexible manipulators," in *Control & Automation, 2007. MED'07. Mediterranean Conference on*. IEEE, 2007, pp. 1–6.

[17] S. Kilicaslan, M. K. Özgören, and S. K. Ider, "Hybrid force and motion control of robots with flexible links," *Mechanism and Machine Theory*, vol. 45, no. 1, pp. 91–105, 2010.

[18] M. Madani and M. Moallem, "Hybrid position/force control of a flexible parallel manipulator," *Journal of the Franklin Institute*, vol. 348, no. 6, pp. 999–1012, 2011.

[19] F. Matsuno, T. Asano, and Y. Sakawa, "Modeling and quasi-static hybrid position/force control of constrained planar two-link flexible manipulators," *IEEE Transactions on Robotics and Automation*, vol. 10, no. 3, pp. 287–297, 1994.

[20] J. Kim, W. K. Chung, and J. Yuh, "Dynamic analysis and two-time scale control for underwater vehicle-manipulator systems," in *Intelligent Robots and Systems, 2003.(IROS 2003). Proceedings. 2003 IEEE/RSJ International Conference on*, vol. 1. IEEE, 2003, pp. 577–582.

[21] A. Ata and H. Johar, "Dynamic force/motion simulation of a rigid-flexible manipulator during task constrained," in *Mechatronics, 2004. ICM'04. Proceedings of the IEEE International Conference on*. IEEE, 2004, pp. 268–273.

[22] T. Endo, F. Matsuno, and H. Kawasaki, "Simple boundary cooperative control of two one-link flexible arms for grasping," *IEEE Transactions on Automatic Control*, vol. 54, no. 10, pp. 2470–2476, 2009.

[23] ——, "Force control and exponential stabilisation of one-link flexible arm," *International Journal of Control*, vol. 87, no. 9, pp. 1794–1807, 2014.

[24] T. Endo, M. Sasaki, F. Matsuno, and Y. Jia, "Contact-force control of a flexible timoshenko arm in rigid/soft environment," *IEEE Transactions on Automatic Control*, vol. 62, no. 5, pp. 2546–2553, 2017.

[25] G. Smoljkic, G. Borghesan, D. Reynaerts, J. De Schutter, J. Vander Sloten, and E. Vander Poorten, "Constraint-based interaction control of robots featuring large compliance and deformation," *IEEE Transactions on Robotics*, vol. 31, no. 5, pp. 1252–1260, 2015.

[26] L. Meirovitch and M. Kwak, "State equations for a spacecraft with maneuvering flexible appendages in terms of quasi-coordinates," *Applied Mechanics Reviews*, vol. 42, no. 11, pp. 161–170, 1989.

[27] A. Ruina, "Slip instability and state variable friction laws," *Journal of Geophysical Research: Solid Earth*, vol. 88, no. B12, pp. 10 359–10 370, 1983.

[28] A. McMinn, A. Pankowskii, C. Ashworth, R. Bhagooli, P. Ralph, and K. Ryan, "In situ net primary productivity and photosynthesis of antarctic sea ice algal, phytoplankton and benthic algal communities," *Marine biology*, vol. 157, no. 6, pp. 1345–1356, 2010.

[29] L. Meirovitch, "State equations of motion for flexible bodies in terms of quasi-coordinates," in *Dynamics of controlled mechanical systems*. Springer, 1989, pp. 37–48.

[30] R. J. Theodore and A. Ghosal, "Comparison of the assumed modes and finite element models for flexible multilink manipulators," *The International journal of robotics research*, vol. 14, no. 2, pp. 91–111, 1995.

[31] S. R. Moheimani and R. L. Clark, "Minimizing the truncation error in assumed modes models of structures," in *American Control Conference, 2000. Proceedings of the 2000*, vol. 4. IEEE, 2000, pp. 2398–2402.

[32] S. Tso, T. Yang, W. Xu, and Z. Sun, "Vibration control for a flexible-link robot arm with deflection feedback," *International journal of non-linear mechanics*, vol. 38, no. 1, pp. 51–62, 2003.

[33] L. Zhang and J. Liu, "Adaptive boundary control for flexible two-link manipulator based on partial differential equation dynamic model," *IET Control Theory & Applications*, vol. 7, no. 1, pp. 43–51, 2013.

[34] C. L. Dym and I. H. Shames, *Solid mechanics*. Springer, 1973.

[35] L. Meirovitch, *Methods of analytical dynamics*. Courier Corporation, 2010.